Understanding Beam Losses in the CDF Collision Hall

Mike Lindgren, Tom Phillips, Rob Roser, Jeff Spalding, Rick Tesarek
For the CDF operations Group

CDF Note 5960

June 2, 2002
V4.0

Abstract:

In this note, we describe a series of tests and look at a variety of detector data in an effort to understand and quantify the size and character of the accelerator related losses in the CDF collision hall. Ideally we would like to identify the cause of the beam loss and feed it back to the accelerator tuners so that they can eliminate or at least minimize this problem. Practically, we will try to quantify in this note how much shielding is required in the CDF collision hall in order to make the current loss rate "tolerable" if the accelerator division is unable to make any further progress.

Observations:

The accelerator-based losses have manifest themselves in many ways. It is fair to say that we are still learning about new effects in our detector and in our readout electronics that are directly attributed to these high losses. Below we describe a few of the more prominent features that we have observed thus far.

- In Run 1 and in the early part of run 2, the anode currents in CMP were small. One HV channel typically handled 12 "stacks" or 48 wires. Nominal current draw for one of these HV channels is 0.5 to 0.7 micro amps. In Run 1, with the exception of the CMP stacks mounted on top of the central detector, there was no correlation between current draw and luminosity. The top stacks had some dependence upon the beam current because of their proximity to the main ring and thus main ring losses. The CAEN HV trips for all of Run 1 were set to 1 microamp. In late August 2001, a few months into Run II, the current draw in the chambers began to rise significantly. Now in a store with luminosity 1-2 x 10^{31}, losses in CMP can be as high as 10 microamps a factor of 20 larger than Run 1 for comparable luminosity.

- On November 25th, the accelerator ran a 150 GeV proton beam into our beampipe wall during collider startup after a prolonged (6 week) access. In this accident, the proton beams collided with the beampipe at the point where our pipe connects up to the Q4 low beta quad magnet on the east side of the collision hall. Nominally this is approximately 100 inches beyond the outermost steel plate in the endplug. Over the course of several hours, single turn proton shots were injected into the machine. During that time period, 12 VME crate power supplies were damaged – 11 on the east side and one on the West. These switching power supplies manufactured by ASTEC were damaged due to SEB (single event burnout). Since that event, we have lost an additional 31 power supplies due to SEB. All of these additional failures have occurred while beam was in the machine; most of them during either injection or scraping. The bulk of the PS failures occur on the West side of the detector, the side that is most susceptible to proton losses.

- The new CDF detector has an unprecedented amount of electronics mounted directly on the detector in order to cope with the increased complexity of the experiment and the ever-increasing demand for faster decision times. As a result, there are lots of programmable logic array chips mounted on these circuit boards. Examples include the silicon fiber interface board (FIB), the calorimeter shower max electronics… Both the silicon and plug groups have found discrepancies in what they thought was stored in their memories and what was actually resident after a store. These corrupted FPGA's make it look as though the hardware is "flaky" and give rise to "bad" channels that come and go (depending upon the memory corrupted). In the short term, this problem is remedied by downloading the information more frequently.

Accelerator Environment

There were many changes made to the accelerator complex between Run I and Run II. The most significant change as far as CDF is concerned is that the Main Injector has replaced the main ring. While this new machine was built to improve the overall luminosity of the machine, it should help our loss situation by removing a source of particle losses from our collision hall.

The second most significant change in the complex is that the accelerator is now operating with 36 bunches as opposed to 6, with new helical orbits. As a result, the higher losses in Run II are not unexpected. Figure 1 shows the predicted spectrum of losses in the Tevatron as a function of position along the ring. The origin of this plot is at the IP in B0. Thus losses in the CDF collision hall can be seen from 6275m (West side of collision hall at the Q3 magnet) and ~15m (East side of collision hall at Q3). These losses did not exist at B0 at this magnitude during Run 1. The leading cause for this new source of losses is the F17 collimator. This newly installed device is 90 degrees in beta away from the B0 low-beta quads. Thus an angular deflection as a result of the beam scraping against the collimator at F17 translates into an excursion in position at B0. e.g.

the beam strikes the beampipe in the Q2 low beta quad magnet and creates a shower of particles inside our collision hall.

In order to quantify the beam loss problem, a series of observations and measurements were made. The next several sections of this note describe in some detail the observations that have been made with regards to beam losses as well as a specific set of measurements that were performed.

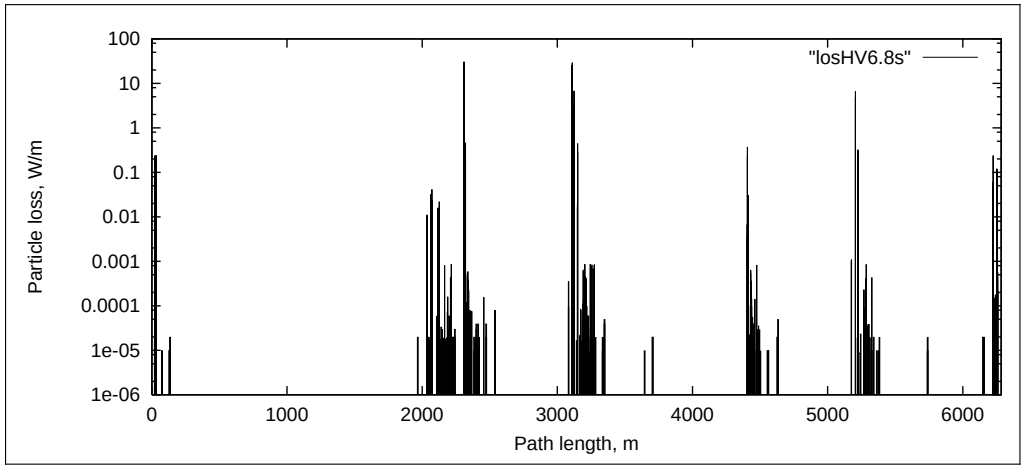

Figure 1: Proton losses in (W/m) as a function of position around the ring. The horizontal axis is in meters from the B0 IP. The spike on the far right edge of the plot is the result of losses hitting Q3 at the WEST end of the CDF Collision hall. This figure is taken from the "Tevatron Run-II Beam Collimation System", FERMILAB-Conf-99/059

Power Supply Failures

Since the start of Run 2 data taking, we have had 43 VME power supply failures in the CDF collision hall. All of these failures have occurred while we were taking beam. Most of the failures occurred during either ramping or scraping – but some were lost during the first 15 minutes into a steady state store. Following the work reported in *SINGLE EVENT BURNOUT IN DC-DC CONVERTERS FOR THE LHC EXPERIMENTS*. By C. Rivetta (Fermilab), B. Allongue, F. Faccio (CERN), G. Berger (Louvain U.), W. Hajdas (PSI, Villigen). FERMILAB-CONF-01-250-E , we have determined that the power supplies failed due to ionizing radiation – through the process referred to as "single event burnout" (SEB). SEB occurs when an energetic charged particle passes through one of the 4 power transistors in the hybrid module while the transistors are fully biased. When this happens, there is insufficient "head room" in the transistors to absorb this additional current and the hybrid circuit fails 100% of the time. There can also be further collateral damage in the power supply circuitry as well.

To confirm that the problem was in fact radiation, we measured the cross section of the transistors used in the hybrid power factor correction module to determine their sensitivity to ionizing radiation. To measure the cross section of these transistors, we (Rick Tesarek and Claudio Rivetta) brought a test setup to the University of Indiana Cyclotron laboratory where we irradiated the Astec power transistors along with some replacement candidates with a beam of energetic protons. In order to obtain sufficient failures to perform a true statistical analysis, they used discrete transistors in a test circuit that was current limited. Thus a "failure" caused by single event upset would only create a small current spike. It would not cause the transistor to self-destruct. The incident beam used was $2x10^8$ p/cm^2/s, of 200 MeV protons. The total irradiation dose for each transistor was $2x10^{11}$ p/cm^2. The resulting cross-section measurements as a function of bias voltage are shown in Figure 2. Note that the ASTEC power transistor that operates at a nominal 400V and is represented by the solid black circles is quite susceptible to this type of damage.

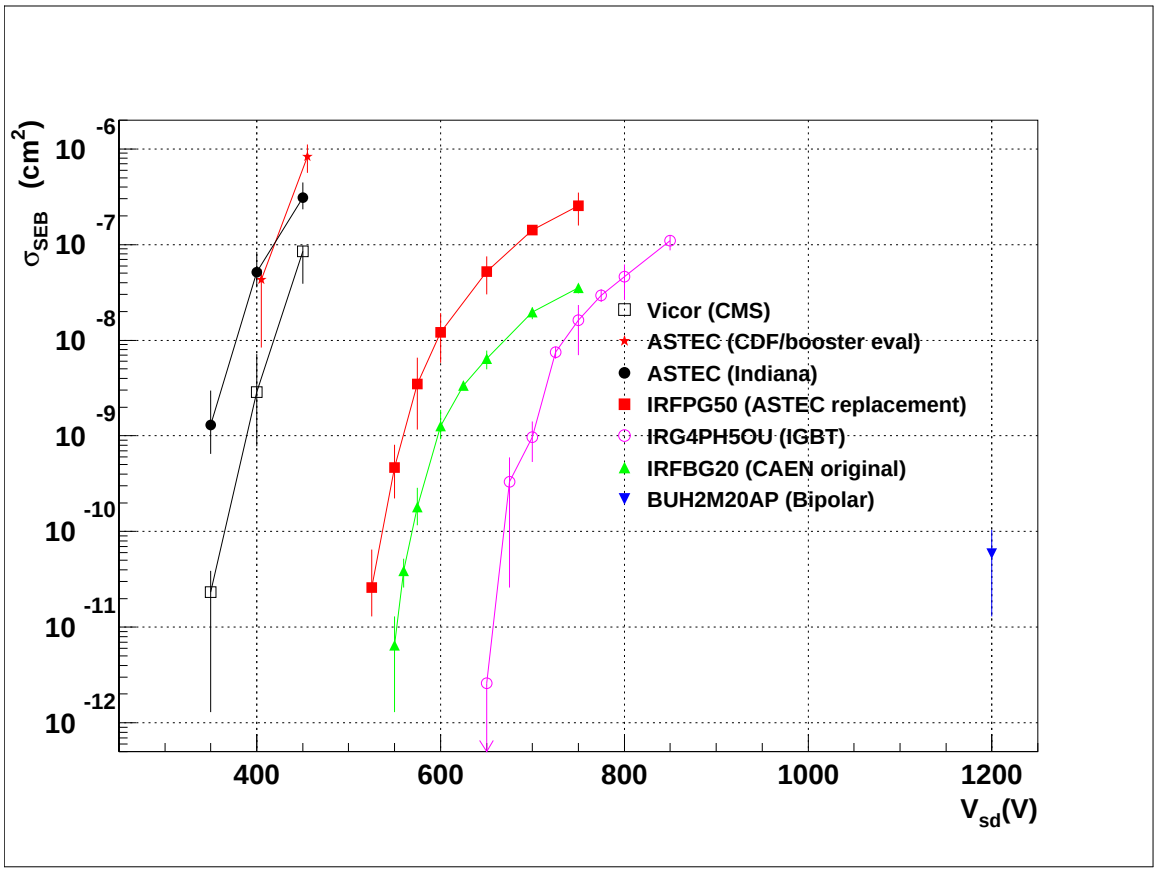

Figure 2: Power Transistor cross-section measurements as a function of bias voltage. The black curve with the circular points is the curve of interest here. That is the MOSFET transistor used in the ASTEC supply. Its nominal operating point is 400V. This plot is courtesy of Rick Tesarek.

Unfortunately, it turns out that we now have gathered sufficient statistics in power supply failures that we can use the physical distribution of failures to show us where we have gaps in our shielding and some characteristics in the nature of the losses. A cartoon sketch of the collision hall is drawn below. Each box indicates a location where one or more VME switching power supplies reside. The numbers adjacent to the boxes indicate the number of power supply failures that have occurred to date at that particular location. (Note that the 12 supplies lost as a result of the beam hitting the beampipe on the east side are **not** included here) From this picture, we see that the two "hot" spots are the NW Bottom Silicon rack and the SW Top COT rack. In both of these locations, there is appreciably less building cement between the rack and the line of low beta quad magnets. It is also interesting to note that there are virtually no failures on the East side, indicating that these losses are coming from the proton side.

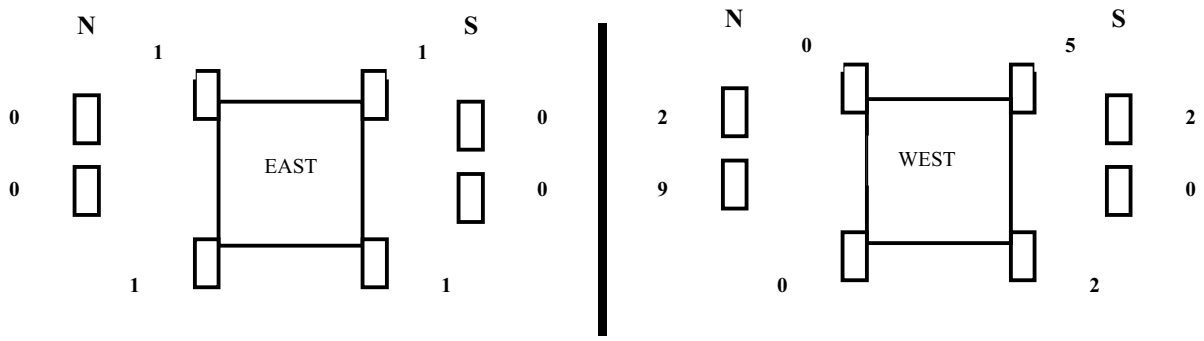

Figure 3 – A cartoon sketch of the CDF collision hall. Each of the small rectangles represents locations of the Astec switching power supplies. The numbers adjacent to these rectangles represent the number of power supply failures at that particular location.

Muon Currents and their dependence on the position of the IMU steel

As a first test to see how effective additional shielding would be at reducing the current seen in the muon chambers, we tracked chamber currents while moving the IMU steel from its running position to its fully withdrawn position (120" back). As shown in Figures 4 and 5, the IMU steel offers little shielding to the CMP chambers when in the running position but offers some shielding when pulled back. Note that these pictures are somewhat misleading because the CMP chambers form a square where as the IMU steel is circular.

The tests were performed on Feb 14th and 15th. Consecutive stores were used to try and keep the beam conditions as close to identical as possible. Figures 6 and 7 show the beam currents (in microamps) for the two configurations of the IMU steel. The muon current readings were taken when LOSTP readings were the same for both stores, namely at 8:00 AM and 4:00 AM respectively.

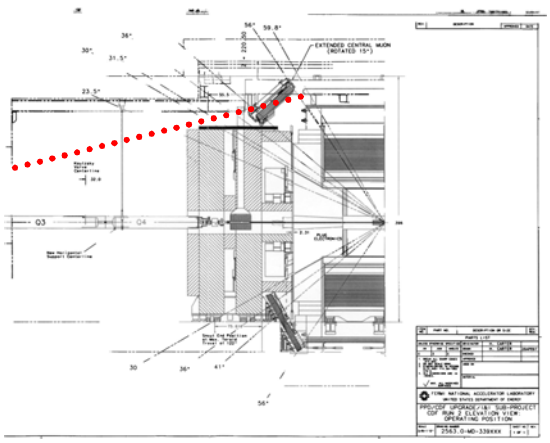

Figure 4: Collision Hall in the nominal running position. The IMU steel is pushed in. Note that there is a line of sight from the low beta quads to the CMP top chambers (dotted red line).

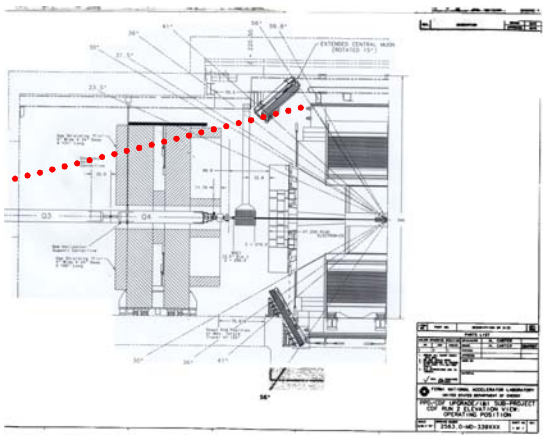

Figure 5: Collision Hall with the IMU steel pulled back its entire 120" travel. This offers some shielding – however due to the circular shape of the steel, it does not offer the full 1-meter of steel shielding.

From Figure 6, we see that the nominal CMP currents range from 0 to 7.5 microamps. The currents are highest in the top corners of the detector. The currents stay high along the top of the detector but fall as you move down either the north or south muon walls. Note that the bottom chambers draw almost no current – presumably a result of the shielding provided by the concrete floor. Thus, if we could either properly shield the losses or get the accelerator division to significantly reduce the losses seen in our collision hall, then based on the CMP Bottom chamber currents, we would expect all of the CMP chambers to return to Run 1 operating conditions.

The map of the current draw for the CMP chambers with the IMU steel pulled back 120" is shown in Figure 7. Immediately we see that with the steel pulled back, the currents in the bottom chambers increased by 3 to 5 fold depending on the channel. Most likely this rise in current is the result of beam halo hitting the miniplug and spraying the endwall. Remember that the "mini-snout" which surrounds the mini-plug is no longer in a position to provide any shielding to CMP. Similarly, the outer snout is of no use in this configuration. The source of losses that result in high currents on the CMP bottom chambers should be isotropic – that is they should be seen equally on ALL CMP chambers. However, this effect (of the miniplug splash) is masked by the already high chamber currents seen everywhere else. The change in chamber current as a result of IMU steel motion is most representative in CMP HV channel 18 (center channel on the

bottom). Remember that channels 16,17, 19 and 20 have an additional block of steel that is welded in front of them that is used to mount the "push-pull" brackets required to physically move the detector into the collision hall. Thus, if we use the 2.3 microamps measured in channel 18 as a pedestal and subtract this value from all channels in Figure 7, the chamber currents from particles upstream of the shielding steel is range from 0 to 3.7 microamps. Therefore, pulling the IMU shielding steel back the 120" resulted in a factor of 2 decreases in the effective chamber currents in CMP. While not an impressive reduction, it is clear that the increase in chamber currents is the result of losses upstream of the CDF detector.

One last piece of evidence that the IMU does provide some shielding, the YMON distribution of hits is consistent with the IMU shadow.

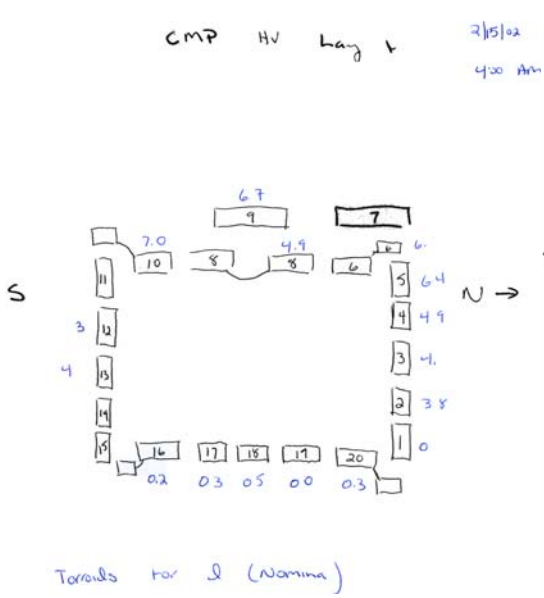

Figure 6 – CMP current map with IMU steel in nominal running condition. All numbers in microamps.

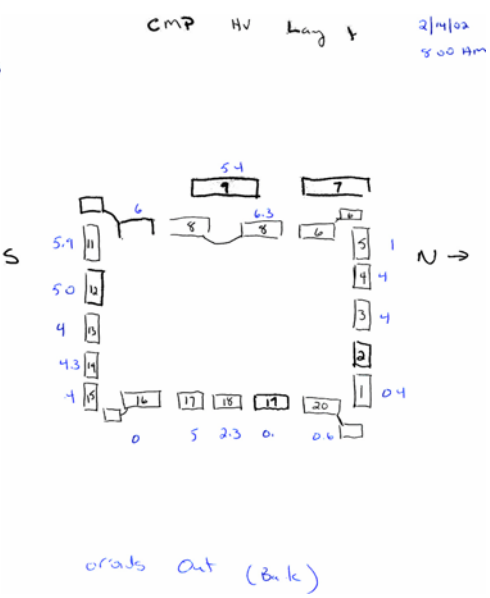

Figure 7 – CMP current map with IMU steel pulled back (away from IP) by 120".

Study with Scintillation Counters in the Alcove

An initial study of the backgrounds in the collision hall by Rick Tesarek (CDF/MEMO/CDF/PUBLIC/5873) indicated that the low beta quads are essentially a line source for a background of charged particles. In order to further understand where these losses were coming from, and to empirically measure the effect of various shielding configurations will have on the muon chamber currents, we built and installed a series of scintillation counter telescopes. Each telescope consists of 2 counters that are 8 inch squares and _" thick. The phototube/base is glued directly to each counter and then wrapped. These telescope (counter pairs) were installed inside the collision hall either in the West alcove or on 13' stands just east of the West alcove. The tall stands were required in this location so that all measurements could be made at beam level.

Figure 8 illustrates in cartoon form the various configurations of these telescopes. The yellow rectangle represents the 6-foot concrete shielding wall that separates our collision hall from the tunnel. The brown rectangle represents a large slab of steel -- approximately 29" thick and 9.5" tall. The two square boxes, tan in color, were used as shielding configuration mock-ups. These boxes were made of steel bricks and were constructed to completely enclose the counters and provide 8 inches of steel shielding on all 4 sides. Note that only one "tan box" was installed for a given test. The closely spaced parallel lines in the figure indicate the location of each telescope (pairs of counters).

The tests consisted of a series of counting experiments with the shielding in a variety of configurations. The two pairs of blue counters were permanently installed. They were not moved for any of the tests described below. A third pair of counters was added at the location of one of the square tan shielding boxes. Data were taken for a given counter configuration with the counters inside the box and then when a second set of data was taken with the box disassembled. (The counters were unshielded but in the same physical location.) For some of the tests the counters were oriented parallel to the beam and the other tests perpendicular to it. The data were arbitrarily normalized to the pair of blue counters closest to the concrete shielding wall.

The results for these tests are noted in the cartoon layout of Figure 8. For instance, the value of 4.5 next to the right-most square box indicates that there was a reduction of a factor of 4.5 (again normalized to the most upstream counters) when the counters were placed inside the steel compared to when the counters were unshielded.

A similar result (factor of 4.0) was obtained when this box was moved from the collision hall into the alcove and the experiment repeated. For counters oriented perpendicular to the magnets, the reduction was less – only a factor of 2.5.

Some observations

- High coincidence rates were observed between pairs of counters that were well separated physically and oriented perpendicular to each other. Hence a significant number of "in time" events are not necessarily the result of an identical particle

traveling in the appropriate direction but the result of an in-time shower of particles – each of which hitting different counters at the same time. So losses measured close to the low beta quad magnets are not the result of high-energy muons traveling parallel to the beam but rather from showers created by the interaction of a proton and the beam pipe.

- The steel shielding was more effective at reducing the counting rates when the counters were oriented parallel to the beamline than they were when oriented perpendicular to it. When a particle interacts with the beam pipe and showers, there is a significant component of low energy isotropic particles produced. Counters parallel to the beam pipe are more sensitive to this cloud of particles than counters oriented perpendicular to it. Since this isotropic cloud is low energy, even 20 cm of steel offers significant reduction in the counting rates.

- For counters placed perpendicular to the beam, the addition of shielding reduced the counting rates by only a factor of 2.5. While the counters in this orientation still see some of the lower energy isotropic spray, they are more sensitive to the higher energy components of these showers that are moving in the direction of the beam. These higher energy particles would require thicker shielding for the same reduction.

- These tests provide strong evidence that a 40cm thick steel shield surrounding the low beta quad magnets would significantly reduce the rate of power supply loss as a result of single event burnout.

- These tests also make it very clear that we cannot simply extrapolate these results to predict what will be the effect of shielding on the muon currents. A separate set of measurements must be made in the location of the CMP in order to get believable results. (discussed in a later section)

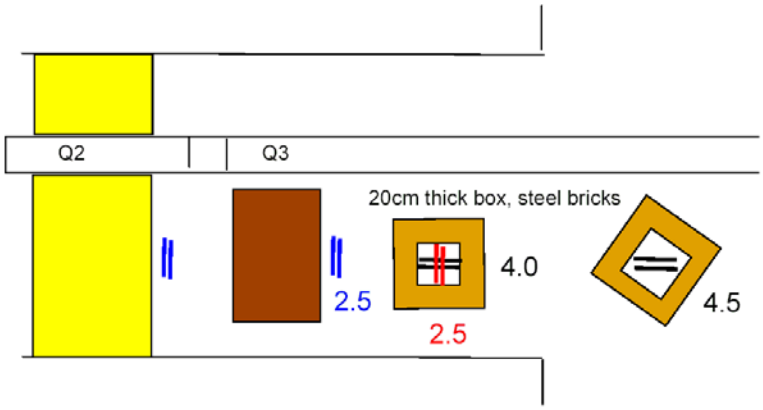

Figure 8: A cartoon plan view of the West most end of the collision hall. The yellow rectangles represent the 6' concrete shielding wall separating our collision hall from the Tevatron. The boxes labeled Q2 and Q3 are in fact the low beta quad magnets. The various sets of parallel lines indicate scintillation counter telescopes whose configurations are described in the text. The numbers represent the reduction in shielding observed by the installation of various steel shielding boxes.

Counters in the Upper Notch

Based on the observations above, it was clear that the only way to know what impact shielding would have at the location where the CMP currents are particularly high. Two pairs of scintillation counters were installed in the "upper notch" of the detector at the same level as the CMP stacks on top west side of the detector. One set of counters was exposed exactly the way CMP is. The second set of counters had 18 inches of steel in front of it. In this case, we did not build a steel box around the counters. The 18 inches of steel was located only in front (west) of the counters. Since the counters are not exactly the same thickness as the CMP chambers, the steel yoke of the central detector provides additional shielding for a portion of the counters.

We took data with the counters in this configuration for several stores and found that the shielding reduced the counting rates by a factor of 200 – 250. We have accounted for the differences in gain between the two sets of counters when making this measurement. Furthermore, for every 1000 particles that we see with identical counters mounted on the 6' thick cement-shielding wall in the West Alcove, we observe 1 particle in the unshielded counters in the upper notch. There is no implied assumption on timing here – rather it's just a statement of fluence. The counters at the CMP chambers are seeing 3 orders of magnitude fewer particles than identical pair of counters located in the West alcove at the cement-shielding wall.

Two final observations can be made. The "back" (east) side of the counters in the upper notch is NOT shielded -- yet we are getting a 200-fold reduction in counting rates. This indicates that the particles interacting with the counters are traveling in a straight path and not part of some collision hall "gas". The closest line of sight point between the alcove

and the low beta quad magnets is at Q2 – inside our cement-shielding wall or on the accelerator side of the shielding wall. The IMU steel shields particles resulting from showers generated closer to the IP.

Timing information in the BMU

Yet another way to quantify the TeVatron losses is to look at the timing information from the BSU scintillators. As a reminder, the BSU detectors are comprised of 6' long pieces of scintillator 6 inches wide that are mounted on top of the BMU muon chambers. Both the BSU and BMU detectors lie on the circumference of the shielding steel formerly known as the toroids. These muon detectors cover about 250 degrees in phi. With the exception of the 6' thick concrete shielding wall that separates our collision hall from the accelerator tunnel, there is no additional shielding between the low beta quad magnets and these pieces of plastic. Dan Cyr and Camille Ginsberg performed an analysis that shows the timing distribution of signals in the BSU scintillator. Two plots from this analysis are shown below in Figure 9. Both plots show the timing for the scintillator while we were taking steady state "physics quality" collisions – the top plot is for the east side detectors and the bottom plot, the west scintillator.

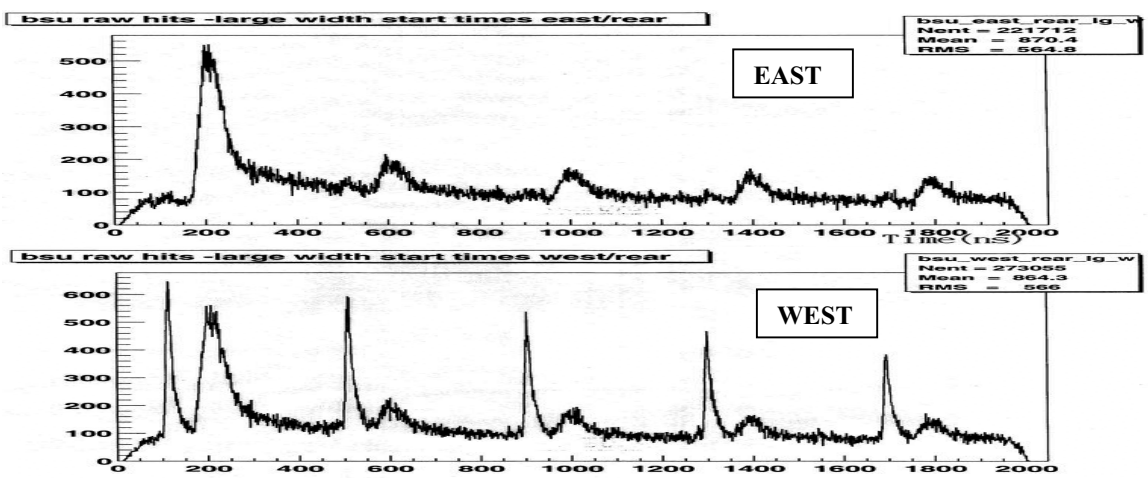

Figure 9: TDC timing distributions for the rear BSU scintillator during steady state collisions on a "typical" set of stores. The top plot is for the counters on the east side of the collision hall and bottom for the west counters.

These plots can be understood as follows: In-time hits from the interaction begin arriving at 155-160ns. Note that these in time hits are in the valley between two loss peaks/processes. Thus most of the hits shown are NOT directly from interactions. This timing was determined (from Dan Cyr and Bob Handler) by requiring a matching track stub and BMU hits. This puts the first peak on the west at about the right time for losses that are in-time with the proton bunch coming from the tunnel or the low-beta quads. We

postulate that the second peak on the west and the large peak on the east come from the "beam jets" resulting from the interaction that triggered this event. These "beam jets" are produced from the spectator quarks in the proton and antiproton that do not participate in the hard scatter. These beam jets proceed down the beam pipe co propagating with the beam bunch until they encounter the first magnet, where the particles in these jets are deflected into the beam pipe. The beam jets then hit the low-beta quads with the resulting showers lighting up the rear BSU counters. In a typical interaction the beam jets will carry most of the energy from the interacting proton and antiproton. Note that the broad peaks are the same size for both the east and the west, which is expected for energy that depends upon the interaction and not upon the beam.

The subsequent peaks come at 396ns intervals from each successive beam crossings. The first broad peak is larger than subsequent broad peaks for both east and west because the triggered crossing is guaranteed to have an interaction that produces beam jets while the subsequent crossings only have interactions a fraction of the time. The sharp peaks from losses before the interaction do not show this same decrease because they only depend upon a proton bunch and not upon an interaction. As the luminosity increases, the size of the broad peak should increase.

The west side clearly shows losses that come before the interaction. (This is the set of "sharp" peaks beginning at about 110ns.) From simple geometric considerations one expects that in-time proton losses should appear in the west roughly 40ns before muons from the interaction. That is, the muons have to travel 40', 20 of it takes you from the counters to the IP and then 20' more for the return trip.

A recent run where the electron lens was off produced the plot shown in Figure 10. Here we see a small peak of losses that precede the interaction on the east side. The histogram for the west during this time period was similar to that shown in Fig. 9.

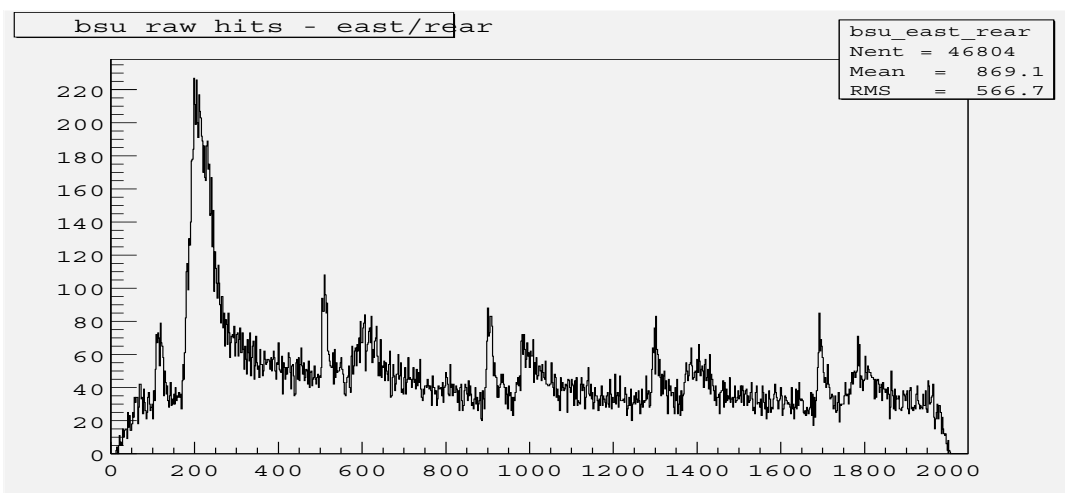

Figure 10: BSU timing on the East Rear scintillator while the electron lens was OFF.

In order to understand whether the source of losses in Figure 9 are the result of interactions away from the central detector or whether they come from the IP, it is instructive to compare the front and rear sections of BSU scintillator. Recall that each BMU stack is shadowed by two pieces of scintillator. Each piece covers approximately 60% of the chamber with a 10% overlap in the middle. We will describe the section of scintillator closest to the IP "front" and the section closest to the low beta quads "rear". Figure 11 shows the timing for hits in the west rear counters (blue) and the front (red). Clearly there are more hits in the rear, which is expected for showers coming sources away from the IP. The peaks for the rear scintillator are earlier in time for the rear (blue) than front (red). This is again consistent with losses coming from the Tevatron side. Finally, while not statistically significant, it is curious to note that the only place where the histogram for the front counters is above the histogram from the rear counters is at 160 ns, which is precisely where real muons from the interaction is expected to be found.

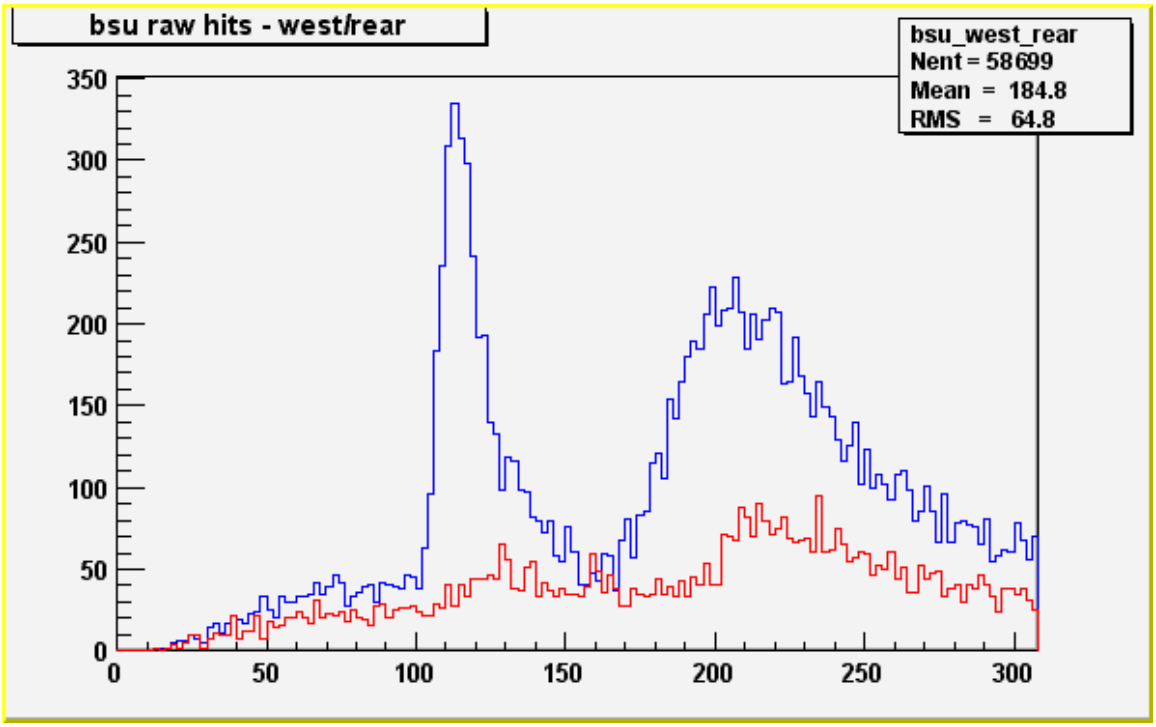

Figure 11: Timing Distribution of BSU hits on the west side of the collision hall. The top histogram (in blue) uses the counters furthest away from the IP. The bottom plot (red) is the timing distribution for the counters closest to the IP. The time is in nanoseconds. In time for this plot is ~160ns.

Conclusions

CDF is currently experiencing much higher losses in the collision hall in Run II than was seen in Run I at comparable luminosity. This increase can be attributed partly to changes in the accelerator lattice, and partly to changes at CDF, specifically moving the toroids forward to expose the low-beta quads. While changing the collimators in the accelerator should reduce the proton losses at B0, CDF will still need protection from beam-loss accidents and from the radiation caused by the beam jets showering in the low-beta quads. We have demonstrated that a moderate amount of steel shielding can significantly reduce the radiation near the low-beta quads. While our greatest exposure from accelerator losses comes from the proton bunches, the priority should be on shielding the west side of the collision hall. However, as the luminosity does increase, the radiation from the beam jets as well as from antiproton losses may be problematic. A shielding plan that is sufficiently flexible such that it can be installed on the east side at a later date is prudent.

To this end, we plan to install temporary shielding in the West alcove during an access of several days in June 2002, and a more complete shield around the quads in the longer access scheduled for October 2002. With the temporary shielding, the quads in the alcove (essentially Q3) will be covered with 18 inch thick concrete blocks. From the tests with the steel brick box, we expect a local reduction of dose in the alcove by about a factor three. The expected reduction at the location of the CMP is not known. In the complete shielding plan, the quads will be surrounded up to the invar support rods by a shield of 40cm thick steel. The design by Stefano Moccia is shown in figures 12 + 13, and is similar to the shield proposed in a simulation study described in *CDF/DOC/MUON/PUBLIC/4532 "CDF Forward Shielding for Run II" by O.E. Krivosheev, N.V. Mokhov*.. From this simulation we can expect an improvement by a factor ten or more in the general radiation levels in the collision hall during normal beam operation.

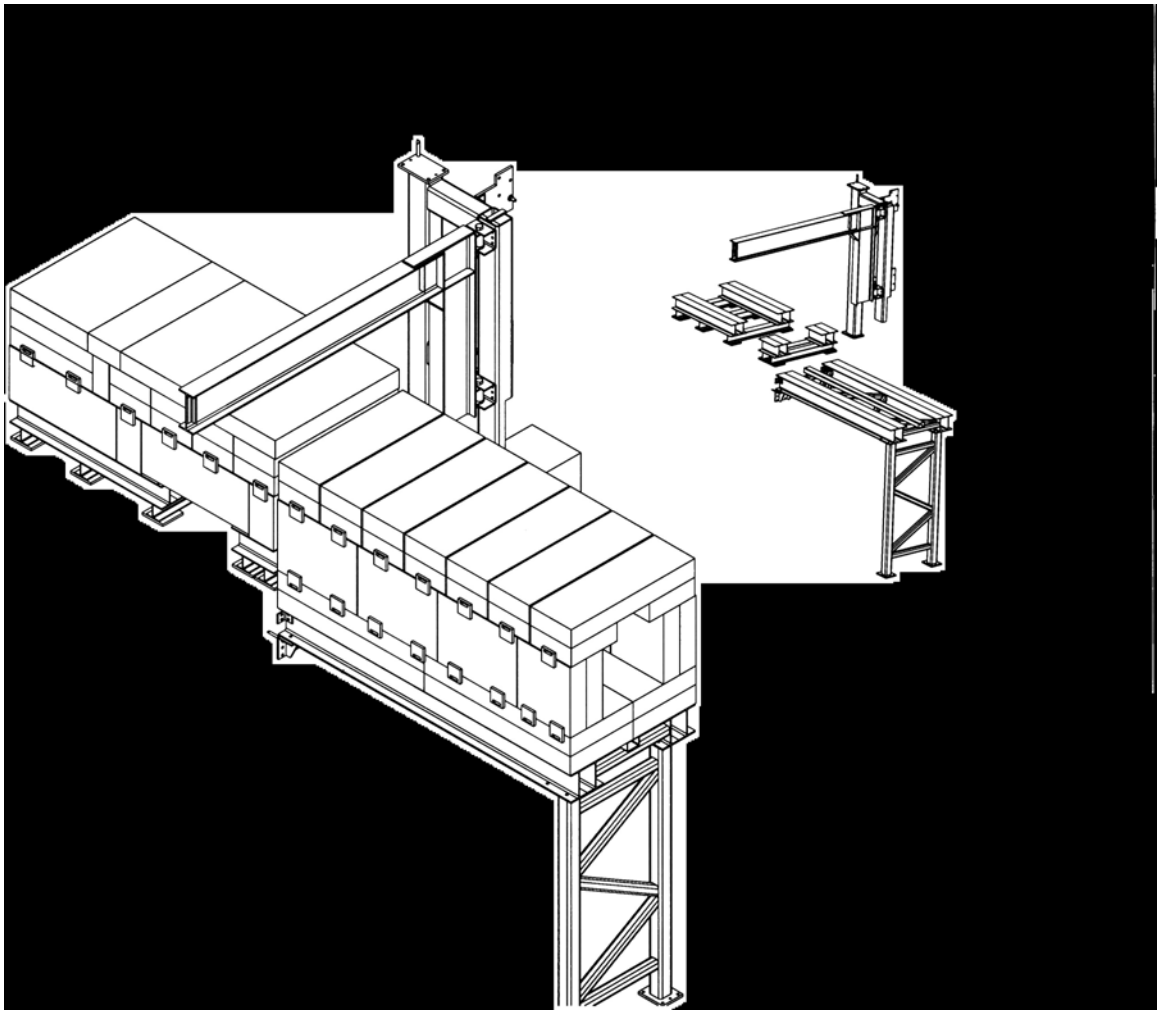

Figure 12: Sketch of shielding plan for CDF's Low Beta Quad magnets. In this sketch beam the IP of the collision hall is to the right. The low beta quad magnets sit inside the steel box. The structure is in two pieces, the left most is the part that sits in the collision hall alcove. The right half forms the bridge in the collision hall. The invar bars supporting the quads are located approximately 1' to the right of this structure. The "arm" sticking out is the crane needed to install these 2800 lb pieces.

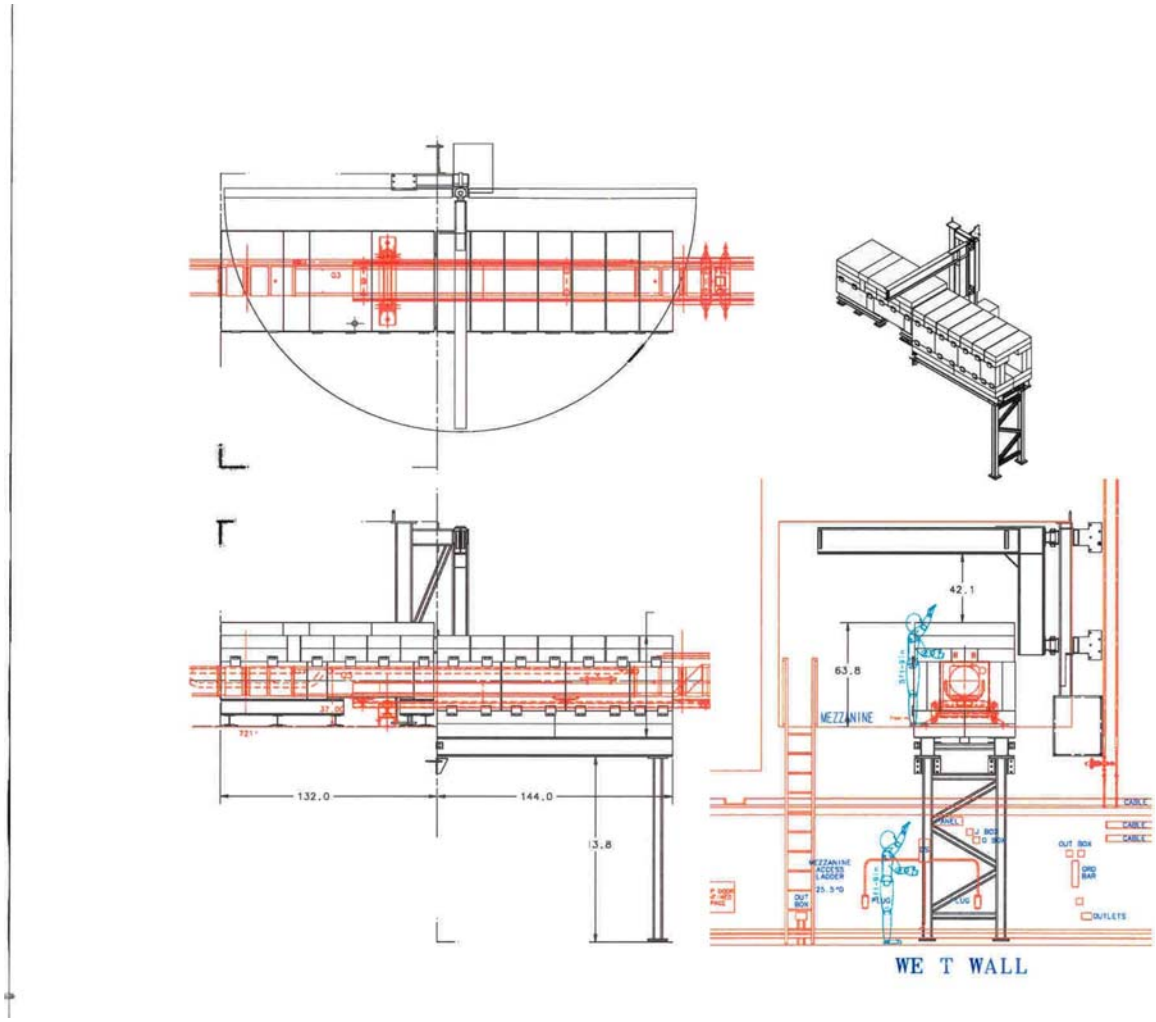

Figure 13: A detailed drawing of the shielding plan for CDF's low beta quad magnets.